Indian Ocean experiments with a coupled model

I. WAINER
Department of Oceanography, University of São Paulo
Praça do Oceanográfico 191, São Paulo, SP - 05508-900 Brazil

(ricevuto il 2 Ottobre 1995; revisionato il 30 Agosto 1996; approvato l'11 Ottobre 1996)

Summary. — A coupled ocean-atmosphere model is used to investigate the equatorial Indian Ocean response to the seasonally varying monsoon winds. Special attention is given to the oceanic response to the spatial distribution and changes in direction of the zonal winds. The atmosphere is modeled using a simple shallow-water system that is coupled to a nonlinear zonally symmetric model, which provides a zonally averaged annual cycle. The Indian Ocean is surrounded by an «Asian» land mass to the North and an «African» land mass to the West. The model extends latitudinally between 41 N and 41 S. The asymmetric atmospheric model is driven by a mass source/sink term that is proportional to the sea surface temperature (SST) over the oceans and the heat balance over the land. The ocean is modeled using the Anderson and McCreary reduced-gravity transport model that includes a prognostic equation for the SST. The coupled system is driven by the annual cycle as manifested by zonally symmetric and asymmetric land and ocean heating. The ocean is driven by atmospheric wind stress forcing and a parametrized heat flux. We explored the different nature of the equatorial ocean response to various patterns of zonal wind stress forcing in order to isolate the impact of the remote response on the Somali current. The major conclusions are: i) the equatorial response is fundamentally different for easterlies and westerlies, ii) the impact of the remote forcing on the Somali current is a function of the annual cycle, iii) the size of the basin sets the phase of the interference of the remote forcing on the Somali current relative to the local forcing.

PACS 92.10 – Physics of the oceans.

1. – Introduction

1˙1. *The annual cycle of the atmospheric monsoon system.* – The annual cycle of the monsoon system over the Indian Ocean is well documented in many climate atlases (*e.g.* Ramage, 1980; Knox, 1983).

These climatologies define a region that possesses the strongest annual variability on the globe. The common elements of both the large-scale winter and summer monsoons include the low-level flow from a large high-pressure area located in the winter hemisphere and the trough located over the land masses of the summer

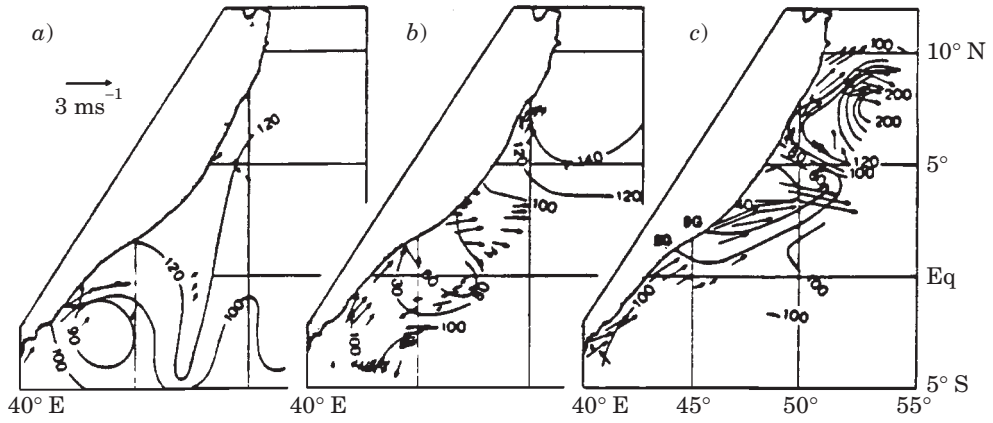

Fig. 1. – Latitude-longitude distribution of the Somali current in May, June and July.

hemisphere. For example, the northern-hemisphere winter monsoon is characterized by a high-pressure zone over Asia (Siberian High) with north or northeasterly flow that crosses the equator converging into the southern hemisphere. As the year progresses, the high-pressure center over Asia weakens, causing the northeasterly winds to decay. At the same time the Mascarene high of the South Indian Ocean intensifies. By July, the winds extend northward across the Indian Ocean toward the heat low that has been established over Asia. The monsoon southwesterlies acquire moisture through evaporation, which is eventually precipitated over the Asian continent. The subsequent release of latent heat is responsible for the vigor of the monsoon.

1'2. *The annual cycle of the Indian Ocean: interaction with the monsoon.* – The Indian Ocean is unique among the tropical oceans because it is forced by seasonally reversing, meridional winds. A direct manifestation of the wind reversal is the near-boundary Somali current off the East African coast. Although the Somali current is essentially meridional in nature, it is also composed of strong eddies, offshore meanders, and recirculations. In contrast to other major western boundary currents, the Somali current changes direction between summer and winter, apparently responding to the general seasonal reversal of the wind field. During the northern-hemisphere summer, the Somali current can attain surface speeds of up to 3.7 m/s (Duing *et al.*, 1980). During the northern-hemisphere winter, the current reverses and weakens to speeds of only about 0.2 m/s (Jensen, 1990). Describing and modeling the evolution of this major boundary current has engaged considerable scientific effort over the years, and has been reviewed by Schott (1987), Knox and Anderson (1985) and Luther (1987). Consequently, only a brief review is presented here.

The seasonal changes of the Somali current (fig. 1) can be briefly summarized. During the northern-hemisphere winter, the northeast monsoon drives a southward boundary current along the coast of Somalia that meets the northward flowing East African Coastal Current off the coast of Kenya.

With the weakening of the winter monsoon, the East African Coastal Current replaces with northward flow the weak southward flowing part of the Somali current. By April or May, with the beginning of the summer monsoon, a northward flow extends

as far as the equator, where the current turns away from the coast to form a meandering eastward flow located south of the equator. In May, the coastal current strengthens and crosses the equator. Part of this current recirculates to the south forming a Southern Gyre that recurs annually. In June, a second gyre appears between 4 N and 8 N and remains quasi-stationary until the summer monsoon winds begin to decay.

1˙3. *Remote vs. local forcing.* – A number of studies have tried to establish the importance of remote *vs.* local forcing in the generation of the Somali current system. Lighthill (1969) explained the onset of the Somali current as a result of accumulating equatorially trapped Rossby waves at the coast. These waves were presumed to be forced remotely by changes in the wind stress curl associated with the onset of the southwest monsoon winds over the central Indian Ocean. The Rossby waves would then travel westward towards the African coast. The time required to establish Lighthill's analog of the Somali current is about one month from the onset of the southwest monsoon. However, other studies indicate that the local monsoon winds along the African coast play a more important role. Cox (1970) for example, points out that the fast spin-up of the Somali current with the onset of the southwest monsoon could only result from the driving force of the local winds. Leetmaa (1972), using ship observations, shows that the Somali current starts flowing northward three to four weeks before the monsoon winds change direction.

With a series of experiments, Anderson and Rowlands (1976) attempted to isolate the roles of local and remote forcing. Their study showed that if both mechanisms were assumed to be of equal strength and switched on simultaneously, the local forcing would dominate initially while the remote forcing would come into play at a later time. They find out that the amplitude of the Somali current increases linearly in time when driven by local winds but quadratically for remore forcing. Cox (1976) found similar distinctions between local and remote effects.

1˙4. *The near equatorial structure of the Indian Ocean.* – Equatorial currents are an important component of the dynamical structure of the Indian Ocean. The most prominent features of the Indian Ocean circulation are an eastward equatorial jet in the central Indian Ocean, first noted by Wyrtki (1973). There is almost never an Equatorial Undercurrent in the Indian Ocean. When it does exist it is due to remotely forced waves. The ocean's response to the uniform and constant wind stress forcing is mostly zonally uniform until coastal influences introduce zonal variations. Easterlies drive a westward surface flow, poleward Ekman flow and upwelling along the equator.

The Indian Ocean has been investigated (modeled) using several layers ocean models in stand-alone mode (*i.e.* externally forced by either observed winds or imposed functions), none of these studies considered the coupled ocean-atmosphere system. The purpose of this study is to examine the evolving structure of the Indian Ocean response to a simulated annual cycle within the context of an interactive and coupled ocean-atmosphere system. We will concentrate on the differentiation of remote and local controls on the structure of cross-equatorial ocean currents at the East African coast. In particular, we are interested in the role of the remote forcing of waves arising from the change in sign of the stress fields in the central and eastern Indian Ocean. We emphasize the generation of these waves, their westward propagation and subsequent trapping at the western boundary. Our aim is to establish the basic physical mechanisms responsible for the interaction

of the ocean response to zonal wind stress with the equatorial Somali current using a coupled ocean-atmosphere model.

2. – Description of the numerical model

The numerical model structure follows the overall design of Anderson and McCreary (1985), with the exception of the atmospheric component that was specifically modified to simulate the effects of the annual cycle. The atmosphere is a linear, shallow-water pertubation model representing an «evolving» steady-state atmosphere linearized about a zero basic state.

The Indian Ocean is surrounded by land masses on its northern and western sides to represent the influences of the annual cycle generated by the zonally asymmetric land masses of Asia and Africa. The specified asymmetric heating arising from the continents is principally responsible for producing the atmospheric monsoon. Physically, the Indian Ocean extends longitudinally for 7500 km. A schematic of the model domain is shown in fig. 2.

The SST, to which the atmosphere is coupled, is predicted by the ocean model. This SST and a prescribed land heating force the atmosphere. The ocean is represented by a reduced-gravity, nonlinear, transport model which is driven by wind stress and by a Haney-type parametrized heat flux (Haney, 1971).

The equations for the model atmosphere are

$$-\beta_y V = -P_x - \varepsilon U\,, \tag{1}$$

$$\beta_y U = -P_y - \varepsilon V\,, \tag{2}$$

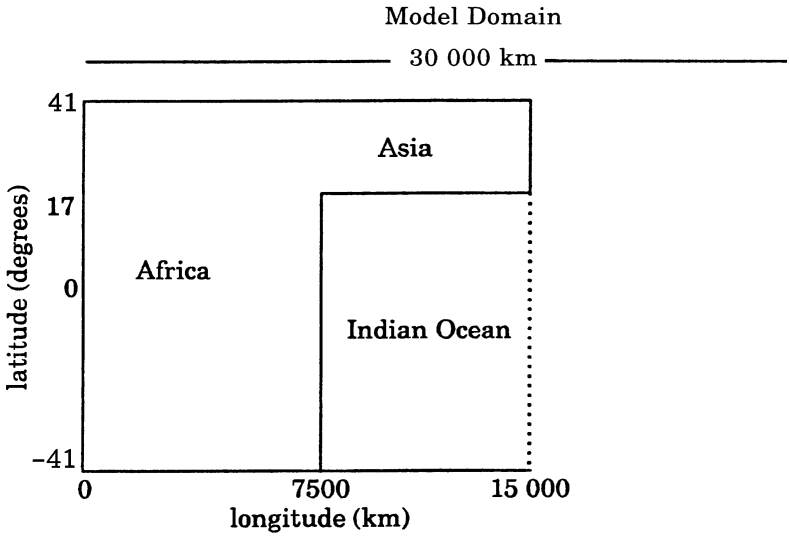

Fig. 2. – Schematic diagram of the model domain. The atmosphere is cyclic in longitude and extends for 30 000 km. The square continental regions simulate the African and Asian continents. The Indian Ocean is 7500 km wide.

$$c^2(U_x + V_y) = Q_T - \varepsilon P \,, \tag{3}$$

$$Q_T = Q_O + Q_L \,, \tag{4}$$

where U and V are the zonal and meridional components of the wind and P is the geopotential. Q_T is the atmospheric forcing, c is the speed of a Kelvin wave, equal to 60 m s^{-1}, and ε is the coefficient of Newtonian cooling, equal to $3 \cdot 10^{-5}$ s^{-1}. These values are the same used by Anderson and McCreary (1985).

Q_O, the latent-heat release over the oceans, is related to SST according to

$$Q_O = Q_o \frac{\mathrm{SST} - (\mathrm{SST})_C}{(\mathrm{SST})_{EQ} - (\mathrm{SST})_C} \Delta(\mathrm{SST} - (\mathrm{SST})_C) \,, \tag{5}$$

where Q_o is an amplitude function, $(\mathrm{SST})_{EQ}$ the temperature calculated at the equator and Δ is the Heaviside step function. Thus the strength of the forcing is proportional to the amount the model-predicted SST is above some critical value.

Q_L, the atmospheric heating over land is a function of time (T) and latitude (ϕ) according to

$$Q_L(T, \phi) = f(T)(f_1(\phi) + f_2(\phi)) \,, \tag{6}$$

$$f_1(\phi) = A \sin\left(\frac{2\pi\phi}{\mathbf{W1}}\right), \tag{7}$$

$$f_2(\phi) = B \sin\left(\frac{\pi\phi}{\mathbf{W2}}\right), \tag{8}$$

$$f(T) = S - \langle S \rangle, \tag{9}$$

$$S = \frac{\pi}{2} \sin\delta + \cos\delta \,, \tag{10}$$

$$\langle S \rangle = \frac{1}{360} \int_T S \, dt \,, \tag{11}$$

where f_1 represents the heating over the model African continent and f_2 the heating over model Asia. A and B are amplitude factors. **W1** and **W2** are the widths of the continental regions. $\delta = \alpha \sin(2\pi/360)$ gives the time dependence. In longitude f_1 and f_2 are forced to have a maximum value at the center of the continental regions and decay linearly towards the continental edge. The number of days in a model year was set to be 360 for simplicity.

The equations for the model ocean, from Anderson and McCreary (1985), are

$$(hu)_t + (huu)_x + (Huv)_y - \beta_y hv = -p_x + \frac{\tau_x}{\varrho} + \nu_h \nabla^2(hu) \,, \tag{12}$$

$$(hv)_t + (huv)_x + (Hvv)_y + \beta_y hu = -p_y + \frac{\tau_y}{\varrho} + \nu_h \nabla^2(hv) \,, \tag{13}$$

$$h_t + (hu)_x + (hu)_y = \frac{2\delta}{hT} - W + \gamma\left(\frac{T - T^*}{T}\right), \tag{14}$$

$$T_t + uT_x + vT_y = \frac{2}{h}\left[-\gamma(T - T^*) - \frac{\delta}{h}\right] + \nu_h \nabla^2(T), \tag{15}$$

$$P = 0.5\varrho\alpha g' h^2 T, \tag{16}$$

where $g' = ((\varrho_{bot} - \varrho_{top})/\varrho_{bot})\, g$.

T is the temperature excess of the surface layer over the bottom layer. ϱ, α and ν_h are the density, thermal expansion coefficient and horizontal viscosity coefficient. The values of these constants are the same used by Anderson and McCreary (1985).

The surface stress is related to the atmospheric fields according to

$$\tau_x = \varrho_{atm} C_D' U, \tag{17}$$

$$\tau_y = \varrho_{atm} C_D' V, \tag{18}$$

where C_D' has the value of 0.008 m s^{-1}. T^* is a function of latitude with a maximum value of 11.33 °C at the equator decreasing to 4 °C at a distance of 4500 km north and south of the equator.

The reader is referred to Anderson and McCreary (1985) for more details on the formulation of the coupled model and its sensitivity to parameters.

3. – Experiments

There is a role for both the local wind stress in the vicinity of the coast and the modifying influence of the remotely forced Rossby waves in determining the annual cycle of the Somali current and the annual cycle of the Indian Ocean, in general.

In order to identify more clearly the manner in which the mid-ocean waves are forced and how they affect the western boundary current, we perform two specific simulations in which the zonal wind stress is externally specified although, at the same time, the meridional wind stress continues to vary as a function of time in the form provided by the coupled model. That is, in each simulation, τ_x is a specified function whilst τ_y continues to be derived from the coupled model. By allowing the ocean to be forced by the same meridional wind stress as in the fully coupled model, an attempt is made to minimize changes in the local forcing in the vicinity of the coast. Changes in the form of the zonal wind stress, on the other hand, allow us to control the remote generation of the Rossby waves. Through this technique, we have a crude understanding of how the remote Rossby waves are generated.

We investigate the equatorial Indian Ocean response to three different types of zonal wind stress distributions in order to understand the relationship between the annual cycle, the generation of the Somali current, and the influence of local and remote wind stress fields. The first case (CP) examines the Indian Ocean response in the fully coupled ocean-atmosphere system. The ocean is initially spun-up by an imposed wind stress that is switched off after 90 model days. The coupled model is then run for 100 years. We look at 36 months of model results starting from year 70, by which the initial transients have decayed and the seasonal cycle has become well established.

The second and third sets of simulations (SC1 and SC2 for semi-coupled) involve two different imposed wind stress distributions in which the coupling between the ocean and the atmosphere is selectively simplified. In this manner, the atmosphere is partially decoupled from the ocean in order to perform controlled simulations to elucidate certain physical processes. The simulations were performed using: i) a zonal wind stress that possessed a uniform spatial distribution and which was allowed to reverse in sign every half year (SC1) and ii) a zonal wind stress distribution that is steady in time and uniform in space (SC2). In both SC1 and SC2 the meridional wind stress forcing, τ_y, is given by the atmospheric component of the coupled model. In this way the meridional component of the wind stress remains fully coupled whereas the zonal component is controlled.

The experimental design presumes the importance of the meridional wind stress in providing the basic character of the western boundary current. The principal aim of the control simulations is to test the importance of the zonal wind stress distribution in producing the propagating Rossby waves along the equator.

4. – Results

To explore the relationship between local and remote forcing and the response of the ocean, the evolution of the ocean flow along the equator is examined in a series of time *vs.* longitude plots. Figure 3 displays time-longitude basin-wide cross-sections of the zonal and meridional wind stress forcing along the equator for a three-year period. During each annual cycle the central and eastern parts of the basin are dominated by westerly wind stress with maximum values occurring in early spring. Next to the

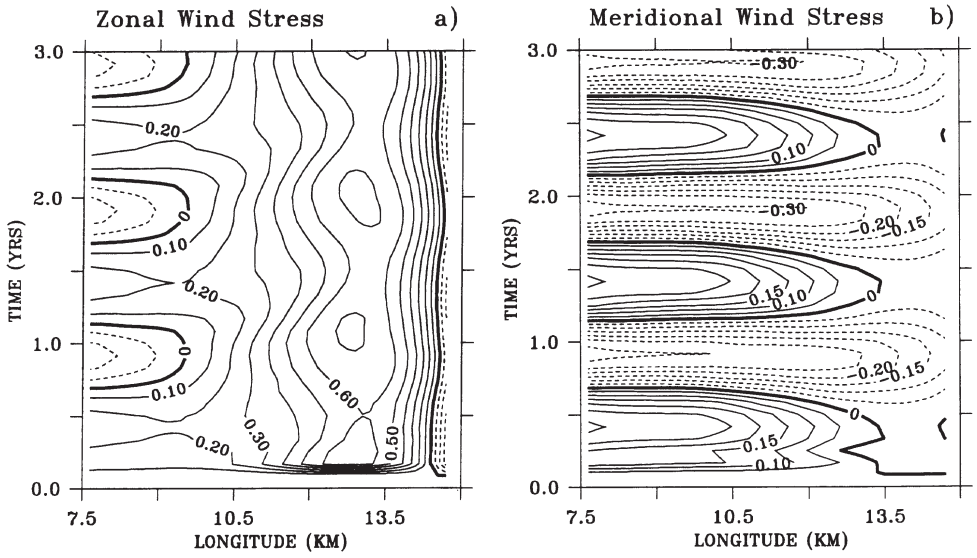

Fig. 3. – Time-longitude distribution of the zonal (*a*)) and meridional (*b*)) wind stress derived from the coupled model along the equator (dynes cm^2). The central-eastern part is dominated by westerly wind stress. Seasonal protrusions of easterly wind stress occur at the western boundary.

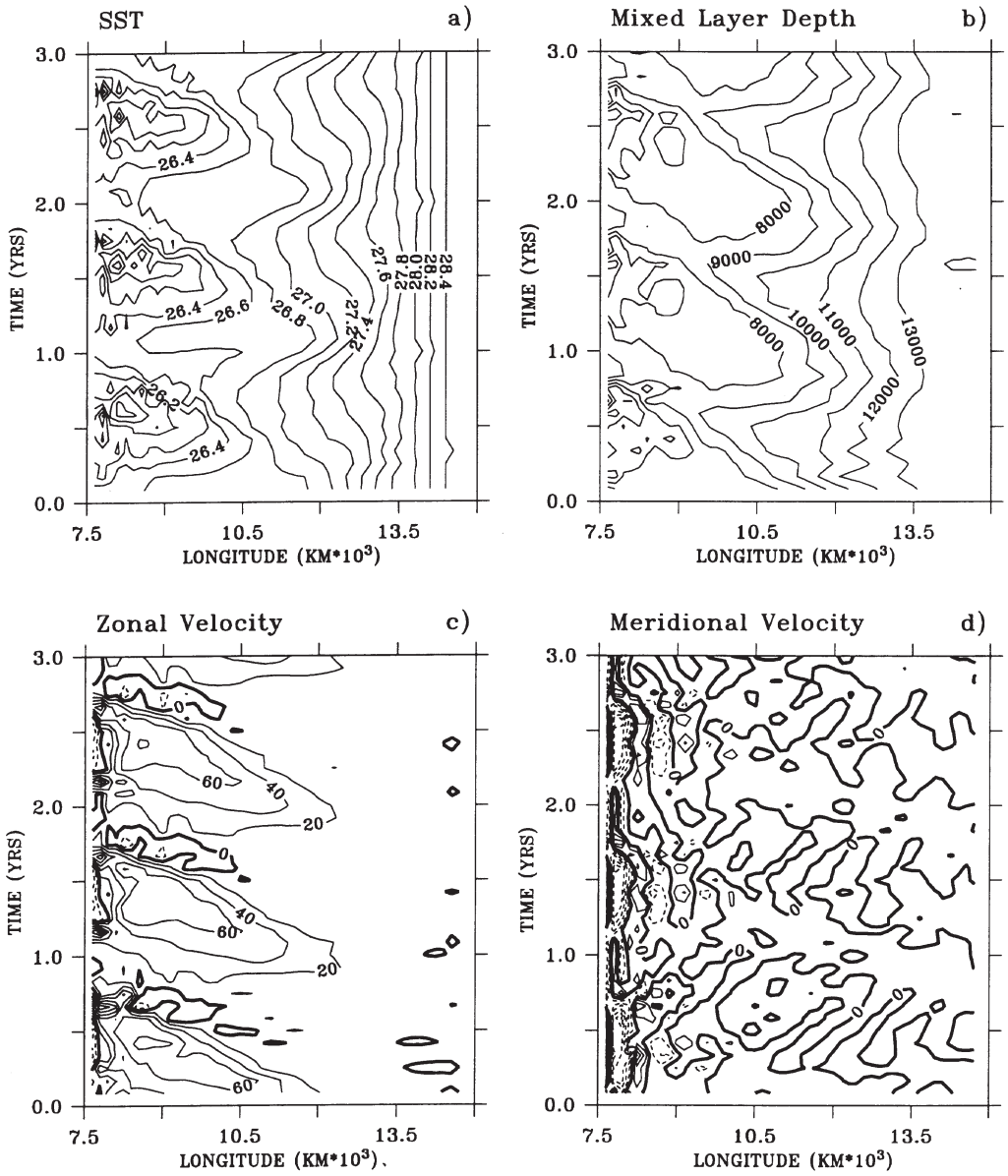

Fig. 4. – Time-longitude distribution of the coupled model along the equator: *a*) SST, *b*) the mixed layer depth (cm), *c*) the zonal current (cm s^{-1}) and *d*) meridional current (cm s^{-1}). A wavy pattern is observed to propagate from the central part of the ocean into the western boundary.

western boundary, seasonal protrusions of easterly wind stress appear that correspond to the monsoonal winds reversal. Thus, in the western ocean in spring, the zonal wind stress changes sign abruptly. The meridional stress shows a very clear annual signal with a maximum northward stress corresponding to the height of the monsoon flow. The seasonal extrema occur against the African coast.

The evolving fields of *h, u* and *v* are shown in fig. 4*a*)-*c*), respectively, for 3 years of integration. Solid lines indicate positive values (*i.e.* either eastward or northward currents). Dashed lines show negative values (westward or southward). The mixed layer depth (fig. 4*b*)) possesses a strong annual cycle with a general east-to-west slope throughout the year. The zonal current field (fig. 4*c*)) along the equator is predominantly eastward from approximately April to October and westward from November to March. We note immediately that the zonal current response is far more complicated than the atmospheric wind stress fields shown in fig. 3. This complexity arises from the anisotropic character of the response of the ocean to variations in the sign of the wind stress along the equator.

Figure 4*d*) portrays the time evolution of the meridional current. The western part of the basin is characterized by a strong seasonally reversing boundary current with a period of about six months. However, the remainder of the ocean exhibits an entirely different character. Between the central and western parts of the ocean, an alternating wave-like pattern is evident that is suggestive of the westward propagating equatorial Rossby waves excited by the stress changes discussed in the last section. Once the wave train has been excited by the alterations in the wind stress in the central ocean, it propagates to the western boundary where it appears to affect the Somali current. To the east of the coast the situation is relatively complex.

The mean monthly resolution of the data makes it difficult to identify the propagation characteristics of the modes and their genesis regions. To help with identification, fig. 4*c*) was replotted using 10-day averaged output. With the higher resolution a clear westward-propagating Kelvin wave marked as K_1-K_1 can be seen in fig. 5. This mode can be readily identified as a Kelvin wave by its equatorial symmetry and the absence of a meridional current field. Furthermore, the phase speed is about 1.4 m/s. Generation of the mode occurs in the fall in the western basin and corresponds to the cessation of the south-west monsoon and the change in sign of the wind stress. A second set of waves, in this case propagating to the west, are marked as R_1-R_1 and R_2-R_2.

R_1-R_1 results from the reflection of the Kelvin mode at the eastern wall (cf. fig. 2). The second mode, originating further to the west, corresponds to the rapid acceleration of the westerly winds in early summer. The modes can be identified as Rossby modes by their propagation sense and speed of their propagation, *i.e.* westward at about 0.4 m/s. Furthermore, the mode possesses a strong signal in the meridional current component at the equator indicating an even mode (*i.e.* $n = 0, 2, \ldots$) that would result from the asymmetric forcing about the equator that may be expected to accompany the monsoon.

4˙1. *Subseasonal time-scales.* – During the FGGE Summer Monsoon Experiment (Summer MONEX), Luyten and Roemmich (1982) found evidence of equatorially trapped modes in the Indian Ocean. The data suggested the existence of both a non-dispersive eastward propagating Kelvin wave and a westward propagating Rossby wave. They also found that the meridional component of the velocity field in the equatorial regions is dominated by a subseasonal oscillation of approximately 20 days that was diagnosed as the manifestation of a mixed Rossby-gravity wave. This high-frequency oscillation has also been reproduced by Luther and O'Brien (1985) and Woodberry *et al.* (1989), using a specified wind-driven ocean model. Luther and O'Brien (1985) speculated that the wave is caused by changes in

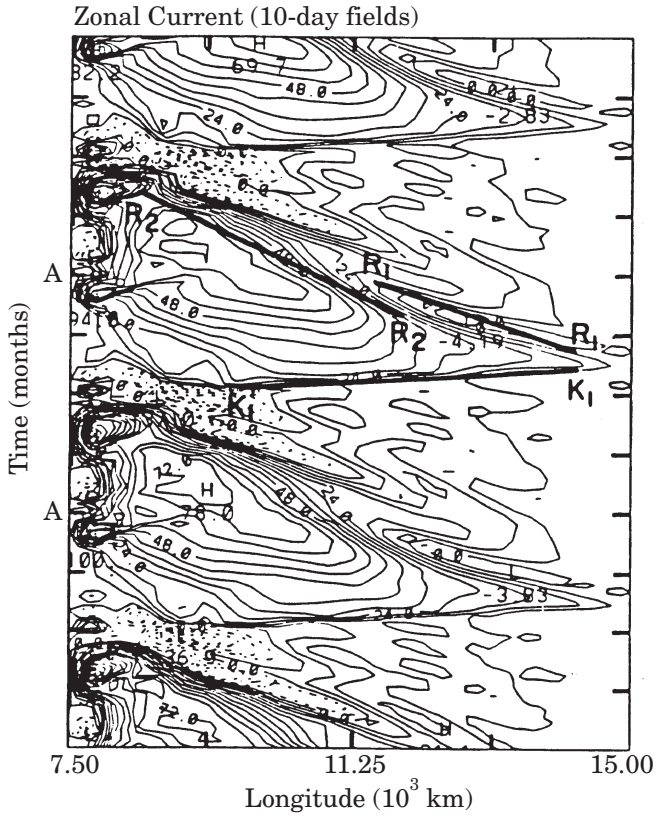

Fig. 5. – Time-longitude section of zonal current using ten-day averaged output. The westward-propagating Kelvin wave is marked as K_1-K_1 on the diagram. Two Rossby waves are marked R_1-R_1 and R_2-R_2.

the ocean structure at the western boundary that acts to transport energy away from the boundary towards the east.

Earlier plots of the ocean structure were not of sufficient resolution to test whether or not a coupled ocean-atmosphere model would produce Luyten and Roemmich's mixed Rossby-gravity mode. Figure 6 displays a time-longitude cross-section of the meridional velocity along the equator plotted every 5 days for the first year of the three-year sample period. The packet may been seen radiating to the east but with a westward phase speed of about 0.25 m/s which is close to the Woodberry *et al.* estimate. Thus, even with the relatively coarse horizontal resolution in the ocean model, the high-frequency behavior of the Indian Ocean annual cycle appears to be well reproduced.

4'2. *Experiment* SC2: *constant zonal wind stress.* – Figure 7*a*)-*c*) shows the evolution of mixed layer depth, zonal and meridional currents for a three-year period along the equator. At the beginning of this period, the zonal stress function was

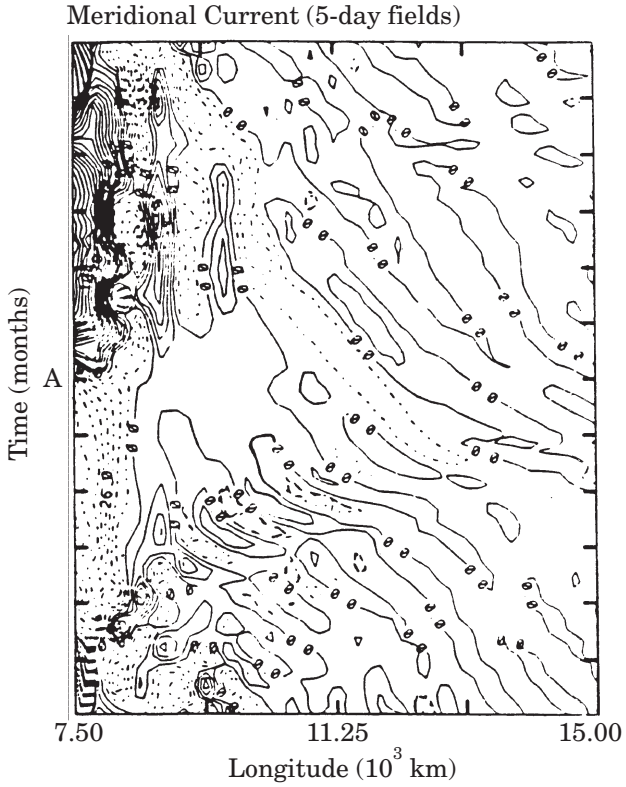

Fig. 6. – Time-longitude distribution of the meridional current, taken every five days from the coupled model along the equator (cm s^{-1}). A very distinct sub-seasonal variability is evident.

changed to the form

$$\tau_x = A \,, \tag{19}$$

where A is a constant set at 0.5 dynes cm^2.

All three fields are very different from their counterparts produced by the fully coupled model. Comparing the SC2 and the CP results (figs. 7 and 4) we find that the response of the meridional velocity component is very simple compared with that of the coupled model. There is also little evidence of Rossby wave propagation from the interior of the ocean.

The mixed layer depth field (fig. 7*a*)) is very flat with only a small amplitude annual cycle. The mixed layer slopes from west to east for the entire year. There is only a weak hint of a propagating signal in the u-field (fig. 7*b*)) from the eastern ocean towards the west. In the SC1 simulation the equatorial zonal currents are very weak. A Somali current is evident (fig. 7*c*)) although the phase is slightly different with the northward current commencing some weeks earlier and lasting slightly longer. The amplitude is

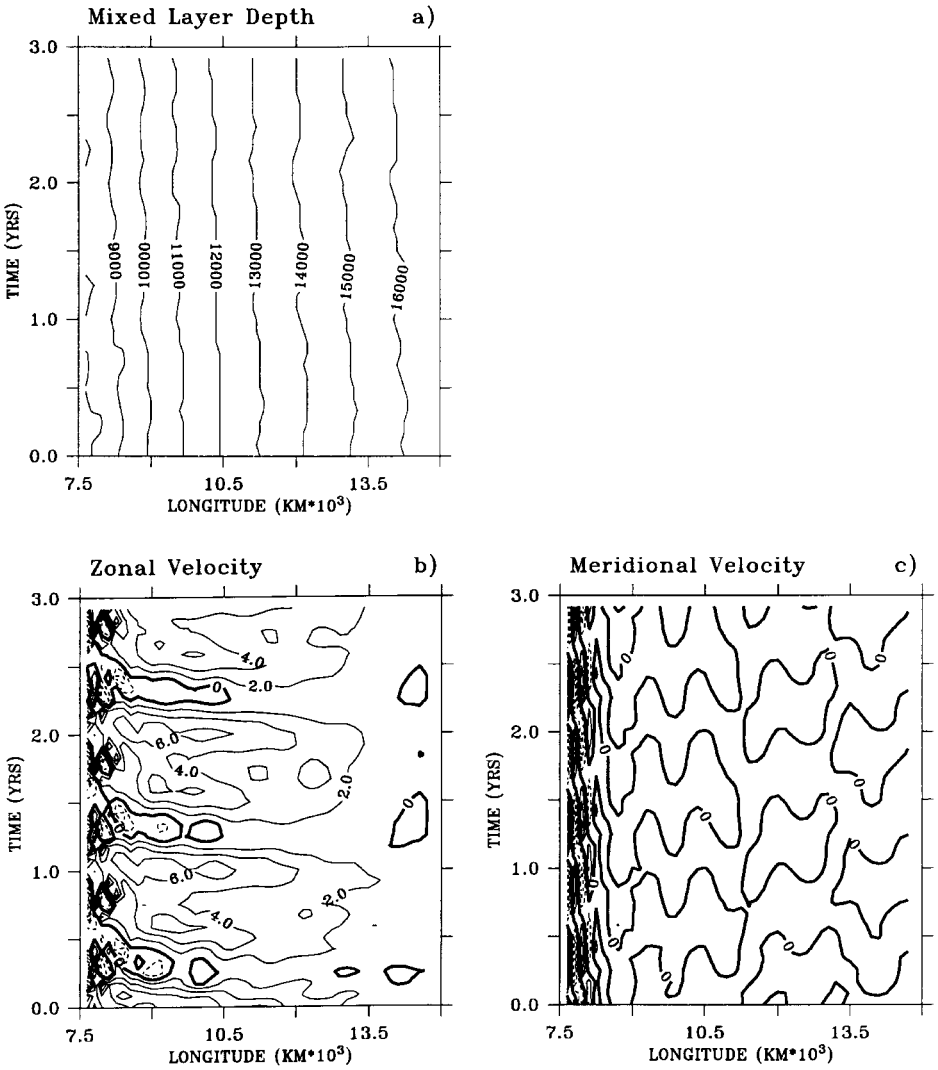

Fig. 7. – Time-longitude distribution for SC2 of *a*) the mixed layer depth along the equator (cm), *b*) the zonal current along the equator (cm s^{-1}) and *c*) the meridional current along the equator (cm s^{-1}).

about a factor of two weaker than in the fully coupled case. There is no evidence of the strong coastal gyres to the east of the Somali current.

The absence of the westward-propagating wave pattern suggests that the remote forcing is clearly linked to the seasonal distribution and variation of the zonal wind stress forcing. Similarly, the differences in the intensity and phase of the western boundary current indicate that, in addition to substantial local forcing, to some degree it is remotely forced.

4·3. *Experiment* SC1: *spatially uniform wind stress.* – The wind stress is set to be uniform in longitude and to vary sinusoidally with time such that

$$\tau_x = A \sin\left(\frac{\pi n}{N}\right), \tag{20}$$

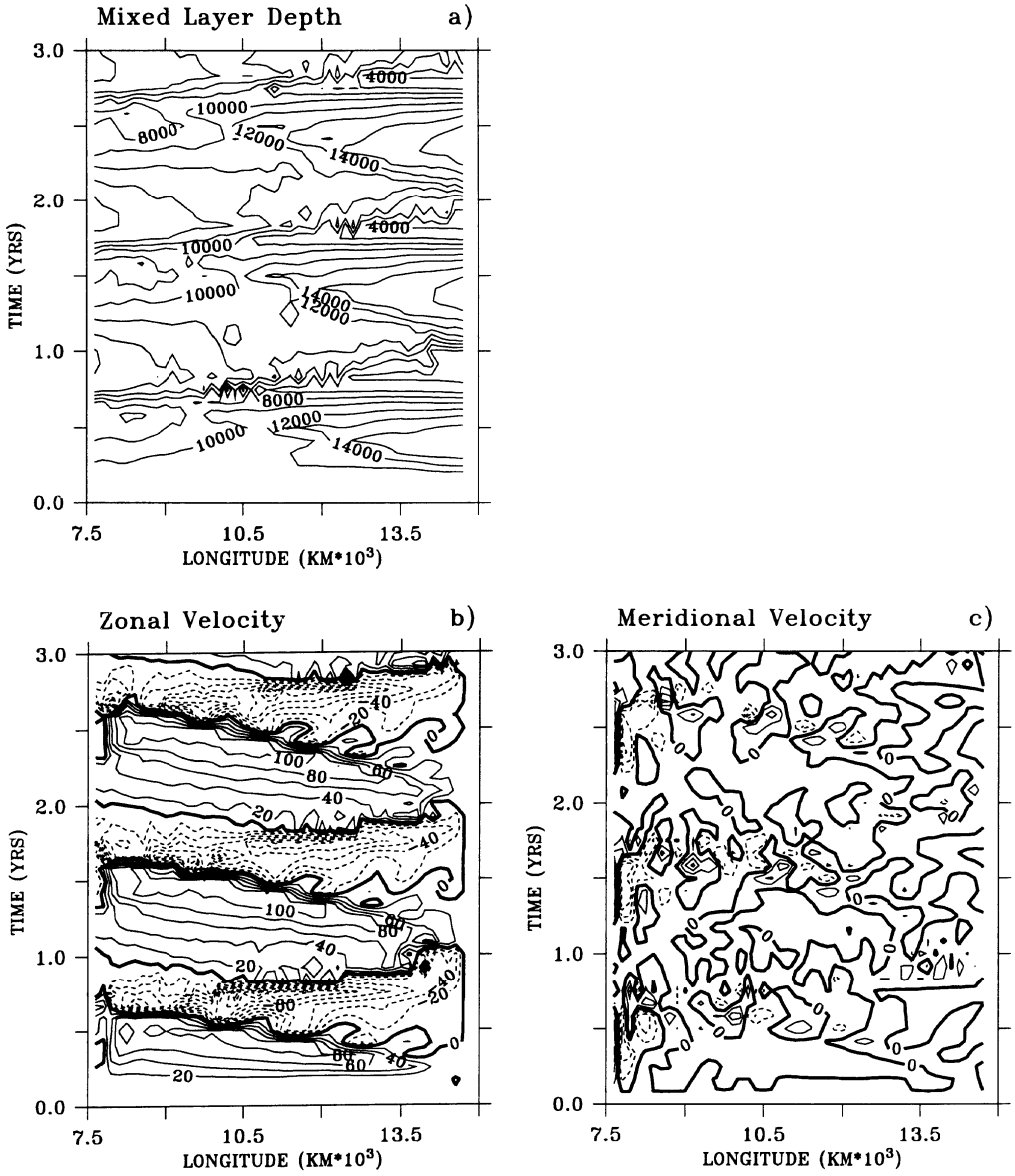

Fig. 8. – Time-longitude distribution for SC1 of *a*) the mixed layer depth along the equator (cm), *b*) the zonal current along the equator (cm s^{-1}) and *c*) the meridional current along the equator (cm s^{-1}).

where A is an amplitude factor, equal to 0.5 dynes/cm^2 and n is the day number. Equation (20) allows the forcing to reverse with a period of N days such that on any day the zonal wind stress is constant along a line of latitude. N is set to give an annual cycle so that τ_x changes sign with a six month period. As in SC2, the meridional stress, τ_y is provided by the atmospheric component of the coupled model.

The significant features are: The annual cycle of the mixed layer depth field (fig. 8*a*)) is quite complicated in the SC1 experiment when compared to SC2 and also different to that produced by the fully coupled model. The gradient now reverses through the annual cycle, whereas in the fully coupled case the thermocline sloped from east to west throughout the year. A similar slope occurs during summer but in winter the tilt reverses. In the SC2 experiment the mixed layer exhibited seasonal variability only in the western part of the domain. There is a clear correlation between the direction of the slope and the direction of the wind stress forcing. A strong summer Somali current is produced that is quite similar in amplitude and form to that found in the fully coupled model except that its northward phase extends about a month longer. However, the southward phase is very much weaker during the early fall and winter. The evolution of the meridional current for the three-year period as in the CP case (fig. 8*c*)) has strong evidence of propagating modes. Unlike the coupled case, they extend completely across the basin.

5. – Summary and conclusions

We have investigated the Indian Ocean response to the seasonally varying monsoon. We explored the different nature of the equatorial ocean response to various

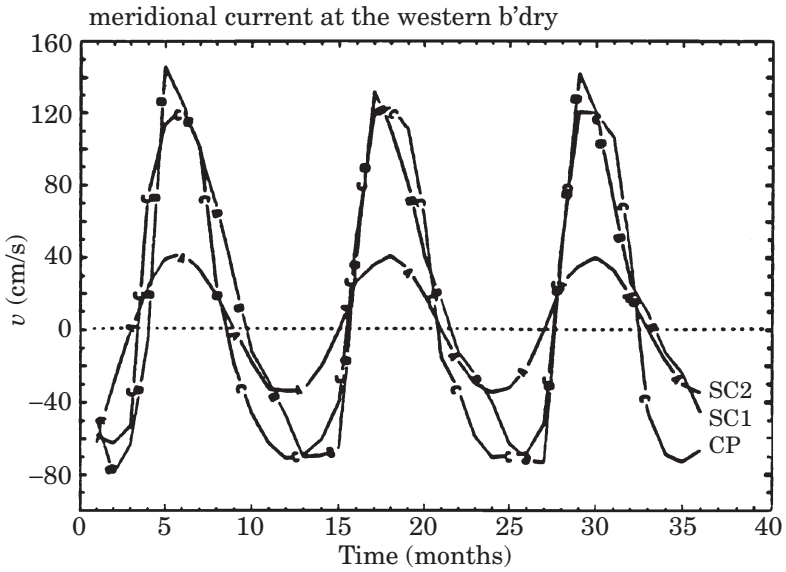

Fig. 9. – Meridional current at the western boundary plotted for each simulation (CP, SC1 and SC2) for the 36-month integration period. The amplitude and phase of CP and SC2 are very similar. With a constant zonal wind stress (SC1) the amplitude of the current is less than half that of the cases with remote forcing.

patterns of zonal wind stress forcing in order to isolate the impact of the remote response on the accompanying Somali current.

The meridional current at the western boundary is plotted for each experiment for the 36 month integration period in fig. 9. Overall, the amplitude and phase of CP and SC1 are very similar. With a constant zonal wind stress (SC2) the amplitude of the current is less than half than that of the cases with remote forcing. This difference indicates that remote forcing is very important in driving the Somali current. However, subtle differences exist between the SC1 and CP cases which have been pointed out previously. The differences indicate the importance of the form of the remote forcing. For example, the zonal scale of the forcing is given by the size of the basin as the Rossby modes appear to be produced at the eastern boundary. On the one hand, the scale of the forcing in the fully coupled case is given by the location of the stress changes which is located in the central Indian Ocean. As the monsoon circulation determines the location of the stress change, the forcing in CP is determined by factors which are north and south of the equator as well. Thus, a variety of factors influence the remote forcing of the Somali current.

The impact of the remote forcing on the Somali current is a function of the annual cycle. If the zonal wind stress does not change directions with time, there is no noticeable remote forcing. The remote forcing enhances the local meridional forcing and the size of the basin sets the phase of the interference of the remote forcing on the Somali current relative to the local forcing.

* * *

This paper was supported by the National Science Foundation under the grant ATM-87-03267, by the United States Department of Commerce under the grant NOAA NA89AA-D-AC015, by FAPESP grant 93/1387-0 and by the National Council for Scientific Research of Brazil under the grant CNPQ 202482/84.

REFERENCES

ANDERSON D. L. T. and MCCREARY J. P., *J. Atmos. Sci.*, **42** (1985) 615-628.
ANDERSON D. L. T. and ROWLANDS P. B., *J. Mar. Res.*, **34** (1976) 395-417.
COX M. D., *Deep Sea Res.*, **17** (1970) 47-75.
COX M. D., *Deep Sea Res.*, **23** (1976) 1139-1152.
DUING W., MOLINARI R. L. and SWALLOW J. C., *Science*, **209** (1980) 588-589.
HANEY R. H., *J. Phys. Oceanogr.*, **1** (1971) 241-248.
JENSEN T. G., *A Numerical Study of the Seasonal Variability of the Somali Current*, PhD Thesis, Florida State University, 1990.
KNOX R. A., *The Indian Ocean: Interaction with the Monsoon*, in *Monsoons*, edited by J. S. FEIN and P. L. STEPHENS (John Wiley and Sons) 1983, pp. 269-330.
KNOX R. A. and ANDERSON D. L. T, *Progr. Oceanogr.*, **14** (1985) 259-317.
LEETMAA A., *Deep Sea Res.*, **19** (1972) 319-325.
LIGHTHILL M. J., *Philos. Trans. R. Soc. London, Ser. A*, **265** (1969) 45-93.

LUTHER M. E., *Indian Ocean modelling*, in *Further Progress in Equatorial Oceanography*, edited by E. KATZ and J. WITTE (Nova University Press, Dania, Fla.) 1987.
LUTHER M. E. and O'BRIEN J. J., *Progr. Oceanogr.*, **14** (1985) 353-385.
LUYTEN J. R. and ROEMMICH D. H., *J. Phys. Oceanogr.*, **12** (1982) 406.
RAMAGE C. S., *Mon. Weather Rev.*, **109** (1980) 1827-1835.
SCHOTT F. M., *Recent Studies of Western Indian Ocean Circulation*, in *Further Progress in Equatorial Oceanography*, edited by E. KATZ and J. WITTE (Nova University Press, Dania, Fla.) 1987.
WOODBERRY K. E., LUTHER M. E. and O'BRIEN J. J., *J. Geophys. Res.*, **94** (1989) 17985-18002.
WYRTKI K., *Science*, **181** (1973) 262-264.